Physical Modelling in Geotechnics

Understanding of microbially induced carbonate precipitation-treated sands by small- and large-strain properties

J.U. Do
Department of Ocean Civil Engineering, Gyeongsang National University, Tongyeong, Korea

ABSTRACT: Microbially induced carbonate precipitation (MICP) is an emerging approach to improving soils' stiffness and strength using bacteria to hydrolyze urea and form calcium carbonate with the presence of calcium source. The MICP-treated sample needs better understanding as the cementation mechanism is different with other types of cemented material such as Portland-cemented, naturally cemented soils, etc. This paper introduces a method using shear wave velocity and cone penetration resistance (K_G) to identify various types of cemented materials. The results indicate that the MICP-treated sands can be differentiated from other cemented soils in correlation with shear wave velocity and cone penetration resistance.

Keywords: MICP, shear wave velocity, cone penetration resistance, mass of calcium carbonate, K_G.

1 INTRODUCTION

Microbially induced carbonate precipitation (MICP) is an innovative method that improves soils' engineering properties using microbes to hydrolyze urea and generate calcium carbonate ($CaCO_3$) when calcium ion is available (DeJong et al., 2010). Micro- to large-scale testing has been used to understand the behavior of MICP-treated soils (Al Qabany et al., 2012; Do et al., 2019; Lin et al., 2017; Montoya et al., 2021; Nafisi et al., 2020; Nassar et al., 2018; van Paassen et al., 2010).

The conventional cementation mechanism based on mixing approach is bonding materials by filling voids via cementation agent (e.g., synthetic cement); however, the cementation mechanism by the MICP process is achieved connecting soil particles by induced calcium carbonate (Cheng et al., 2013; Terzis & Laloui, 2019). In this regard, the evaluation of MICP-treated soils needs special approaches.

In this paper, the parametrization on MICP-treated sands was attempted with respect to the small-strain property (shear wave velocity), the large-strain property (cone tip resistance), and the level of cementation (mass of induced calcium carbonate). A large-scale soil box was used to treat submerged sands with MICP. The shear wave velocity and cone tip resistance were correlated in terms of mass of calcium carbonate. The results indicate the combined properties of MICP-treated sands differ from other types of cemented sands.

2 MATERIAL AND METHODS

2.1 Soil Box and Sample Preparation

A large-scale soil box (0.91 m × 0.91 m × 0.91 m as width × length × height) was used in the experiment. The soil box is submergible with two water reservoirs located at each perforated end of the box (Fig. 1).

Fig. 1. Large-scale soil box.

Silica sands classified as poorly graded sand were air-pluviated in the soil box. The box was filled with water from the bottom of the soil box to simulate a submerged condition. After the inundation, the relative density was computed as 38-42%.

2.2 Treatment

A PVC pipe measuring 5 cm in diameter (D) was installed at the center of the soil box. The pile has perforated surface to a depth of 4D below the surface. The perforations were covered with porous plastic to prevent the surrounding sands from engineering into the pile. The end of the pile was rubber-plugged so

cementation solutions into the inner pile can be infiltrated through the perforations.

The cementation process consisted of six times of 1 biological injection and 3 cementation injections. The biological solution was made of 0.333 M urea, 0.374 M ammonium chloride, and 0.15 *l* bacterial suspension per 1 *l* of media. The bacterial suspension was prepared by ATCC 1376 growth media with ATCC 11859 *Sporosarcina pasteurri*. The growth media incubated in shaking incubator at 30°C and 200 rpm until the optical density at 600 nm reached 0.8-1.2 (Feng & Montoya, 2015). The cementation solution consisted of 0.333 M urea, 0.374 M ammonium chloride, and 0.25 M calcium chloride dehydrate. The treatments were conducted with varying the duration and applied head for approximate 30 days (Fig. 1) (details in Do et al. (2021)).

2.3 Assessment of Small-Strain Property

The representative small-strain property in this study is a shear wave velocity (V_s). The V_s was measured using piezoelectric bender element sensors. Several bender element pairs were embedded within the sands in the soil box (Fig. 1). A 10 V sinusoidal wave was generated by a function generator (Agilent 33522A) and received by an oscilloscope (Agilent MSO6014A). The V_s was calculated dividing the senor's tip-to-tip distance by the first arrival time of the propagated signal. After the completion of the treatment, V_s were measured at each section of the sands.

2.4 Assessment of Large-Strain Property

The presentative large-strain property herein is a cone penetration resistance (q_t). A miniature cone penetrometer was installed above the soil box setup. The penetrometer measured 1 cm in diameter and 60° cone tip. Due to the limited length of the cone penetrometer, a depth of 25 cm from the surface was investigated. After the completion of the treatment, the cone was penetrated near V_s measured to correlate.

2.5 Assessment of Cementation Level

After conducting the cone penetration test, specimens were collected near V_s and q_t measured. The collected specimens were oven-dried and washed by hydrochloric acid to dissolve the induced precipitation. The mass ratio of reduced mass over sand mass gives the mass of calcium carbonate (m_c) in percentage.

3 RESULTS

3.1 Cementation Profile

Although the cementation profile by m_c was obtained after V_s and q_t measurements, m_c profile is explained first to better the understanding of V_s and q_t profiles. The locations of the measurement was normalized by the pile diameter. A single section of the measurements is shown in Fig. 2 assuming axisymmetric changes. Most representative m_c profile among several sections is presented in Fig. 2a. Pre-treatment m_c was 0%.

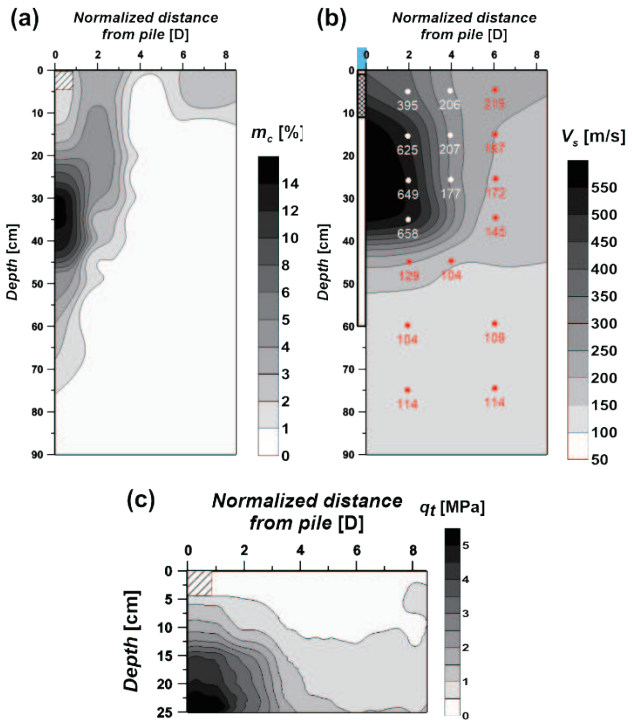

Fig. 2. Profiles after the MICP treatment. (a) Cementation profile, (b) shear wave velocity profile, and (c) cone tip resistance profile.

The cementation profile shows a spherical shape with respect to the injection port as the injection took place in spherical. In general, the level of cementation near the injection source showed a light level of cementation as m_c = 0.2-1.1% at the 5-15 cm depths. At the depth range of 7.5-17.5 cm showed m_c = 0.7-1.4%. Then the cementation increased at 25 cm to 45 cm depths (max. m_c ~ 16.2%). Then the attenuation of m_c was observed below a depth of 50 cm. No perceptible cementation was found below a depth of 85 cm.

The measurement infers that the precipitated minerals were washed away from the injection source at near surface. However, the density effect of the precipitates seems occurred at deeper depth. For radial direction, the cementation happened along the direction of the flow. Near the boundary (e.g., the normalized distance of 6-8D), the accumulation of the precipitates may be occurred.

3.2 Shear Wave Velocity Profile

Figure 2a presents V_s contour after the treatment. Pre-treatment V_s were 61-102 m/s with varying depths due to the effect of different overburden stresses (Santamarina et al., 2001). Due to the spatial limitations of installed instrumentation, some profile exaggerates the improvement pattern; however, the V_s improvement (Fig. 2b) is very well-matched with the m_c profile (Fig. 2a). The improvement occurred with respect to the injection

source. The maximum V_s (658 m/s) was measured at a depth of 35 cm at where the highest m_c (16.2%) was measured.

3.2 Cone Penetration Profile

Pre-treatment q_t showed nearly zero resistance at 0-5 cm depths, and gradually increased up to approximately 0.5 MPa at a depth of 25 cm. In spite of the limited evaluation depth, post-treatment q_t (Fig. 2c) indicates good correspondence with m_c and V_s. The q_t at 2D increased linearly at 0-13 cm depths and 5 MPa showed at a depth of 17 cm. At 1D distance, the highest q_t was observed 7.1 MPa at 25 cm depth. The general q_t profile showed spherical with respect to the injection source like m_c and V_s.

3.3 Correlations of Properties

Schneider & Moss (2011) proposed an empirical parameter called K_G in correlation with V_s and q_t. The K_G includes the combined relationship between the small-strain property (i.e., V_s) and large-strain property (q_t). The K_G is defined as Eq. (1):

$$K_G = \frac{G_0/q_t}{q_{t1N}^{-0.75}} \qquad \text{Eq. (1)}$$

where, G_0 is initial shear modulus as computed by ρV_s (ρ: saturated unit weight of soil), q_{t1N} is stress-normalized cone tip resistance as defined by $(q_t/p_a)\cdot(p_a/\sigma'_{vo})^{0.5}$ (p_a: atmospheric pressure, σ'_{vo}: effective overburden pressure). Following the recommendation by Robertson & Wride (1998), $(p_a/\sigma'_{vo})^{0.5}$ is fixed to be 2 due to the low overburden pressure of the experimental system.

The comprehensive K_G chart including naturally cemented, Portland-cemented, and Gypsum-cemented sands is shown in Fig. 3. Holocene uncemented sands were measured as $110 < K_G < 330$, while cemented and calcareous sands showed $330 < K_G < 1100$ as observed by Schneider & Moss (2011). The K_G values of 2% Portland-cemented sands fit into the range of $330 < K_G < 1100$ (Eslaamizaad & Robertson, 1997). The K_G values of 0-0.5% and 0.5-2% m_c by MICP-treated sands corresponds to the range. The K_G values of 5% Gypsum-treated sands can correlate to ~2500 (Lee et al., 2011). MICP-treated sands with roughly m_c ~2-4% are matched with ~2500 K_G. The correlation is magnified for higher level of m_c. The K_G values of 10% Gypsum-treated sands are located within the K_G range of 5000-7000. However, ~5000 K_G can correlate to MICP-treated sands with 4-5.5% m_c.

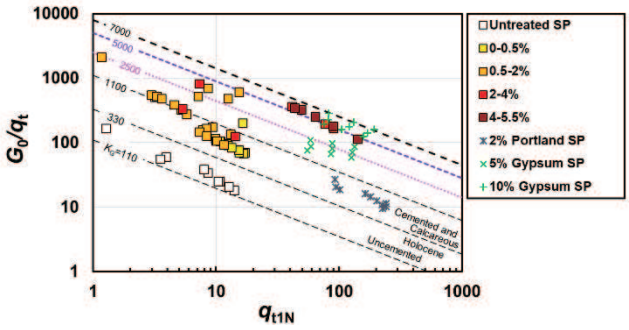

Fig. 3. K_G chart of MICP-treated sand with other types of cemented sands. Data of '2% Portland SP' are from Eslaamizaad & Robertson (1997), and data of '5% and 10% Gypsum SP' from Lee et al. (2011).

The correlation indicates that for similar K_G, the level of cementation by the MICP treatment is generally lower than mixing-based cemented sands (e.g., Portland- and Gypsum-cemented sands). This is because of different cementation mechanism of MICP phenomenon with other types of cementation. MICP induces the cementation of materials via connecting soil particles with calcium carbonate at the particle contact points and surfaces rather than filling the entire void space (DeJong et al., 2010). Portland- and Gypsum-induced cementation (based on mixing method) causes strength and stiffness improvement via filling the void space of the soil system. Correspondingly, it can be said that for same level of cementing agent, MICP-cemented sands have a higher efficiency to improve soils' stiffness and strength compared to artificially cemented sands.

4 CONCLUSIONS

MICP-treated sands were comprehensively evaluated in terms of small- and large-strain properties with level of cementation. The K_G value was used to quantify the properties. Mixing-based cemented sands using Portland and gypsum were compared with MICP-treated ones. The K_G values revealed that MICP treatment method induces effective improvement than other mixing-based cementation due to different cementation mechanism. Therefore, K_G can be a useful indicator to differentiate MICP-treated sands with other types of cemented sands.

ACKNOWLEDGEMENTS

This research was supported by Basic Science Research Program through the National Research Foundation of Korea (NRF) funded by the Ministry of Education (2021R1I1A3049493).

REFERENCES

Al Qabany, A., Soga, K., & Santamarina, C. (2012). Factor s Affecting Efficiency of Microbially Induced Calcite Pr ecipitation. *Journal of Geotechnical and Geoenvironment*

al Engineering, *138*(8), 992–1001. https://doi.org/10.1061/(ASCE)GT.1943-5606.0000666

Cheng, L., Cord-Ruwisch, R., & Shahin, M. A. (2013). Cementation of sand soil by microbially induced calcite precipitation at various degrees of saturation. *Canadian Geotechnical Journal*, *50*(1), 81–90. https://doi.org/10.1139/cgj-2012-0023

DeJong, J. T., Mortensen, B. M., Martinez, B. C., & Nelson, D. C. (2010). Bio-mediated soil improvement. *Ecological Engineering*, *36*(2), 197–210. https://doi.org/10.1016/J.ECOLENG.2008.12.029

Do, J., Montoya, B. M., & Gabr, M. A. (2019). Debonding of Microbially Induced Carbonate Precipitation-Stabilized Sand by Shearing and Erosion. *Geomechanics and Engineering, An International Journal*, *17*(5), 429–438. https://doi.org/https://doi.org/10.12989/gae.2019.17.5.429

Do, J., Montoya, B. M., & Gabr, M. A. (2021). Scour mitigation and erodibility improvement using microbially induced carbonate precipitation. *Geotechnical Testing Journal*, *44*(5). https://doi.org/10.1520/GTJ20190478

Eslaamizaad, S., & Robertson, P. K. (1997). Evaluation of settlement of footings on sand from seismic in-sity tests. *50th Canadian Geotechnical Conference*, 755–764.

Feng, K., & Montoya, B. M. (2015). Influence of confinement and cementation level on the behavior of microbial-induced calcite precipitated Sands under monotonic drained loading. *Journal of Geotechnical and Geoenvironmental Engineering*, *142*(1), 04015057. https://doi.org/10.1061/(ASCE)GT.1943-5606.0001379.

Lee, M. J., Choo, H., Kim, J., & Lee, W. (2011). Effect of artificial cementation on cone tip resistance and small strain shear modulus of sand. *Bulletin of Engineering Geology and the Environment*, *70*(2), 193–201. https://doi.org/10.1007/s10064-010-0312-0

Lin, H., Suleiman, M. T., Jabbour, H. M., & Brown, D. G. (2017). Bio-grouting to enhance axial pull-out response of pervious concrete ground improvement piles. *Canadian Geotechnical Journal*, *12*(June), 1–12. https://doi.org/10.1139/cgj-2016-0438

Montoya, B. M., Do, J., & Gabr, M. A. (2021). Distribution and Properties of Microbially Induced Carbonate Precipitation in Underwater Sand Bed. *Journal of Geotechnical and Geoenvironmental Engineering*, *147*(10), 04021098. https://doi.org/10.1061/(ASCE)GT.1943-5606.0002607

Nafisi, A., Montoya, B. M., & Evans, T. M. (2020). Shear Strength Envelopes of Biocemented Sands with Varying Particle Size and Cementation Level. *Journal of Geotechnical and Geoenvironmental Engineering*, *146*(3). https://doi.org/10.1061/(ASCE)GT.1943-5606.0002201

Nassar, M. K., Gurung, D., Bastani, M., Ginn, T. R., Shafei, B., Gomez, M. G., Graddy, C. M. R., Nelson, D. C., & DeJong, J. T. (2018). Large-Scale Experiments in Microbially Induced Calcite Precipitation (MICP): Reactive Transport Model Development and Prediction. *Water Resources Research*, *54*(1), 480–500. https://doi.org/10.1002/2017WR021488

Robertson, P. K., & Wride, C. E. (1998). Evaluating cyclic liquefaction potential using the cone penetration test. *Canadian Geotechnical Journal*, *35*(3), 442–459. https://doi.org/10.1139/t98-017

Santamarina, J. C., Klein, K. A., & Fam, M. A. (2001). *Soils and Waves*. Wiley and Sons.

Schneider, J. A., & Moss, R. E. S. (2011). Linking cyclic stress and cyclic strain based methods for assessment of cyclic liquefaction triggering in sands. *Geotechnique Letters*, *1*, 31–36. https://digitalcommons.calpoly.edu/cgi/viewcontent.cgi?article=1298&context=cenv_fac

Terzis, D., & Laloui, L. (2019). A decade of progress and turning points in the understanding of bio-improved soils: A review. *Geomechanics for Energy and the Environment*, *19*, 100116. https://doi.org/10.1016/j.gete.2019.03.001

van Paassen, L. A., Ghose, R., van der Linden, T. J. M., van der Star, W. R. L., & van Loosdrecht, M. C. M. (2010). Quantifying Biomediated Ground Improvement by Ureolysis: Large-Scale Biogrout Experiment. *Journal of Geotechnical and Geoenvironmental Engineering*, *136*(12), 1721–1728. https://doi.org/10.1061/(ASCE)GT.1943-5606.0000382